Journal of Rock Mechanics and Tunnelling Technology (JRMTT)
25 (2) 2019 pp 89-102

Available online at www.isrmtt.com

Estimation of Source Parameter of Local Earthquake in Tehri Dam Site and Vicinity

*D. Shanker**
Abhishek Pathak

Department of Earthquake Engineering
Indian Institute of Technology Roorkee, Roorkee, India

**E-mail: dayasfeq@iitr.ac.in*

ABSTRACT

The objective of this study is to estimate hypocentre parameters and source parameters of local events recorded at the seismological laboratory of IIT Roorkee by deploying 12 seismological stations network around Tehri dam region. Hypocentre parameters of 3 local events occurred around Tehri dam region are estimated using the HYPOCENTER program given in SEISAN software. Earthquake source parameters are estimated by using the code EQK_SRC_PARA, in which source model is fitted in displacement spectra and acceleration spectra. For the Tehri dam region, source parameters of small sized local earthquakes ($1.3 \leq Mw \leq 3.2$) are also estimated. The seismic moments (M_0), Brune stress drop and source radii ranges from $2.2x10^{18}$ to $6.6x10^{20}$, 1 to 63 bars and 65.1 m to 667.4 m, respectively. The maximum stress drop of 63 bars is observed at a source radius of 146.7 m. The radiated seismic energy varies from $1.1x10^{14}$ to $3.9x10^{16}$. The radiated seismic energy follows the relationship with seismic moment as $E_s = 3x10^{-5}M_0^{1.013}$. Study indicates that the seismic moment shows the increasing trend with increase in source radius.

Keywords: Source parameters of local events; Hypocenter parameters of local events; Tehri Dam site.

1. INTRODUCTION

The Tehri dam site is located in the CSG region of Himalaya and constructed across Bhagirathi River. The region around Tehri dam site is identified by the occurrence of moderate to large earthquake activity. The objective of this study is to estimate hypocentre parameters and source parameters of local events recorded at the seismological laboratory of IIT Roorkee. An earthquake consists of a large number of parameters. In order to estimate these parameters, a mathematical formula is used that can calculate the hypocenter parameters. The noise parameters have also been used that can calculate the seismic phase and the arrival time of the pulse width in the P and S waves, respectively, in the time and frequency domains.

1.1 Time Domain Method

O'Neil and Healy (1973) calculated the source parameters of local earthquakes by adopting this method. It is the time component between the start of P-wave and the initial zero intersection in the short-term seismic record. It depends on the quality factor of the medium and response of the recording tool. This method overcomes the problems associated with sections of seismogram because of its high frequency and amplitude limitations.

1.2 Frequency Domain Method

Any physical phenomenon that varies not only in space but also in time, it is important to know the rate of its change with frequency. This is achieved by converting the signal from time domain to a frequency domain termed, as the spectrum of the signal. Since convolved signals in the time domain are multiplied signals in the frequency domain, scientific operations are easier to apply in the frequency domain than in the time domain.

2. METHODOLOGY

2.1 General

Earthquake seismic movements show the impact of sources, seismic pathways, site conditions, and instrument responses. The particle displacement path u (x, t) is expressed as the space time convolution of the slip function in the time domain. The signal in the time domain is multiplied several times in the frequency domain. In other words, the analysis in the frequency domain is much simpler than in the time domain. Fast Fourier Transform (FFT) is used to change the signal from time domain to frequency domain.

2.2 Earthquake Models

The development of various mathematical models for earthquake occurrence is described in Nakano (1923). Brune (1970) assumed the theory of a circular source model. In this model, he assumed a tangential stress pulse applied in the direction of the potential surface. The previous potential model was used to determine the displacement through any slip function. Later, Brune (1970) introduced a model used to calculate the displacement of a fault. According to Brune, ground motion parameters are a function of effective stress.

2.3 Procedure Adopted for Data Analysis

The source parameters in this study are determined using the software EQK_SRC_PARA (Kumar et al., 2013a). The calculation consists of following two steps:

(i) Estimation of the observed spectrum from a recorded time series of earthquakes, and
(ii) Calculation of the source spectrum from the observed spectrum.

2.3.1 Computation of the Observed Spectrum

The rotation of the N-S, E-W, and vertical components is performed to calculate the observed spectra from the components of the recorded ground motion using azimuth and incidence directions.

2.3.2 Computation of Source Spectrum

The following equation represents the observed spectrum as:

$$A_i(R,f) = Si(f).P(R,f).S_f(R,f) \quad (1)$$

Ai(R, f) refers to the observed spectrum, $S_f(f)$ refers to the source spectrum, P(R, f) refers to the path spectrum and Si (f) is the site spectrum.

2.4 Earthquake Source Parameters

2.4.1 Seismic Moment

Size and strength analysis of earthquake movements is performed by estimating seismic moments. To calculate the seismic moment, Aki (1966) introduced the following expression:

$$M_o = \mu D A \quad (2)$$

where,

μ - shear modulus of medium,
D - mean final displacement after rupture and
A - rupture surface area.

Keiles-Borok (1959) presents the following relationship to calculate seismic moments.

$$M_{0-} = 4\pi\rho R\beta^3\Omega_0 / SaR_{\theta\phi} \quad (3)$$

where,

R - the distance from the source of the earthquake source to the earthquake station,
ρ - the average density of the medium around the source,
β - S wave velocity of the medium around the source,
$R_{\theta\varphi}$ - the correction applied to the radiation pattern,
Ω_0 - S-wave spectrum amplitude at low frequency, and
Sa - amplification correction due to free surface effect.

2.4.2 Source Radius

The radius of the circular fault is estimated using the following equation:

$$R = 2.34\beta/2\pi f_c \quad (4)$$

where,

- corner frequency and
- shear wave velocity

2.4.3 Stress Drop

The stress drop is the difference in average stress across a fault back and fore of earthquake. The stress drop is given by-

$$\Delta\sigma = c\mu D/L \quad (5)$$

where,

D - the avg slip of fault area (A),
L - the characteristic length of the fault area,
μ - the elastic shear modulus and
c - a geometric constant.

2.4.4 Average Displacement

The displacement mean value of the fault plane can be calculated as follows.

$$D=M_0/\mu A \quad (6)$$

3. STUDY AREA AND ITS TECTONICS

The dam is located at the intersection of the Bhagirathi and Bhilangana rivers, 640 meters above the msl (Fig 1). The reservoir has an area of 44 km^2 to Bhagirathi and a length of 25 km to Bhilangana valley. The Tehri Dam is about 5 km in the south direction of the North Al-Molar Thrust (NAT) (Choudhury et al., 2013). NAT appears to have moved around 500 meters by tipping NE-SW on Dewal Tear, which is a transverse fault situated in the Bhilangana river valley. NW-SE, including Gadolia Tear, which is a strike slip fault, moves in the parallel direction to NAT in a similar valley and eventually converges to NAT. The NW-SE slanting Tehri Tear has an opening in the Jalkur River, which is on the tributary of the Bhagirathi river, and continues to run over around 10 km upstream of the Bhilangana river (Choudhury et al., 2013). The E-W slope, including the Marh Tear, is about 4 km downstream from the dam (Choudhury et al., 2013).

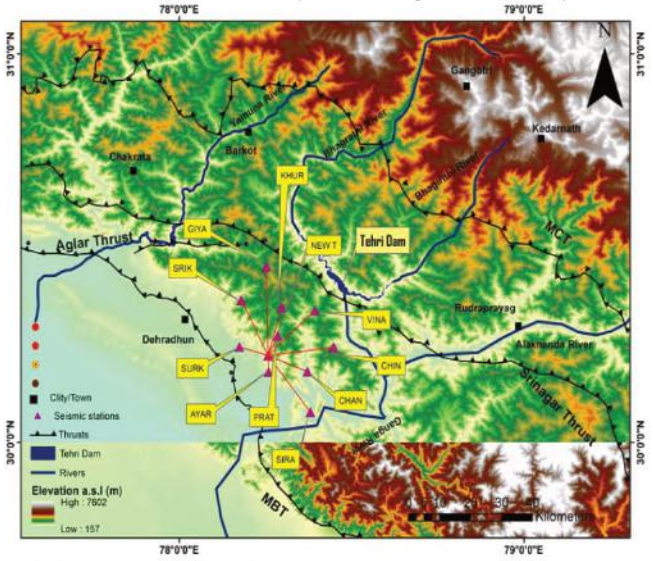

Fig. 1 - Study area with location of recording stations along with epicentres of local earthquakes

Authors checked the emissions of the two channels at Uttarkashi (Bhagirathi river) and Ghansali (Bhilangana river). The influx of two rivers was found somewhere between 20 and 1600 × 106 m^3 on September 20, 2010. The minimum scaling level Minimum Draw Down Level (MDDL) of the store is at 740m msl. The water level record was used to associate the seismic information around the dam.

3.1 Seismicity Around Tehri Dam

The site of the dam is identified in the 700 km long earthquake gap in between the 1905 Kangra earthquake in the west and the 1934 Bihar-Nepal earthquake in the east. However, the other major earthquakes in the past destroyed the plate boundary of just 200 to 450 km, leaving no rupture in the middle of the earthquake gap. The collapse of the Himalaya between the faults (along which rupture occurred) of the Kangra and Bihar earthquakes is called the Himalayan seismic gap (Sengupta, 2010). Tehri Dam is in the gap of this earthquake. The real concern is not the magnitude of the earthquake that occurred in the region over the last 200 years, but the progress of the Tehri dam (Gaur, 1993).

A study on seismic activity at Tehri Dam was carried out in two different seismic movements. First, there is a pseudo-ground acceleration (Mw =7) of the earthquake (PGA= 0·23g) used in the dam design. The second is the earthquake of non-existent magnitude (Mw = 8.5) and a physiological

earthquake acceleration (PGA = 0.45g). The second hypothetical action in nature is the Maximum Credible Earthquake (MCE) in the Tehri dam area specified by Sengupta (2010). This has caused numerous conflicts among experts on the approval of these two movements. The correct method is to perform the PSHA in an area of 500 km within the source of the earthquake.

4. DATA ANALYSIS

4.1 Estimation of Hypocenter Parameters on 24 January 2015

The phase data of 3 earthquakes are recorded at 12 seismological stations using digital seismograms. The P and S-wave arrival time data of these earthquakes was also measured by the strong motion records. These phase-data of both P and S-wave are collectively used for computing the hypocentre parameters. The velocity model (Table 2), incorporated in computing the hypocentre parameters. For locating the local data, HYPOCENTER computer program (Liennert et al., 1986), is used and the related estimations have been done by using the software SEISAN (Havskov and Ottemoller, 2000).

Table 1 - Details of the recording stations of the network

S. No.	Station Name	Station Code	Geographical Coordinates		Elevation
			Latitude	Longitude	
1	Ayarchali	AYAR	3018.22'N	7825.91'E	2108
2	Rajgadhi	RAJG	3024.59'N	7844.70'E	1906
3	Giyanja	GIYA	3045.34'N	7825.26'E	2122
4	Srikot	SRIK	3036.77'N	7817.93'E	1621
5	Khurmola	KHUR	3034.81'N	7829.68'E	1733
6	Binakkal	VINA	3033.99'N	7839.33'E	1633
7	Pratapnagar	PRAT	3027.48'N	7828.55'E	2123
8	Surkanda	SURK	3024.67'N	7817.34'E	2720
9	New Tehri	NEWT	3022.42'N	7825.77'E	1903
10	Chintarbaghi	CHIN	3024.59'N	7844.70'E	1946
11	Chanderbadni	CHAN	3018.31'N	7837.15'E	2252
12	Sirala	SIRA	3007.92'N	7838.03'E	1408

Table 2 - Velocity model for local events

P-wave velocity (km/sec)	Depth to the top of the layer (km)
5.56	0.0
6.10	10.0
6.45	20.0
6.90	30.0
7.60	40.0
8.40	50.0

Table 3(a) - Hypocenter parameters estimated from 12 Seismic stations for local event recorded on 01 January 2015

St. Code	Geographical Coordinates		Depth (km)	Mw	Epic Dist (km)	Hypo (cm)	Azi
	Latitude	Longitude					
Ayar	3018.22'	7825.91'	6.09	2.6	61.7	6.2E+06	170.3
Rajg	3024.59'	7844.70'	0.12	2.2	8	8.0E+06	.263.6
Giya	3045.34'	7825.26'	0.15	2.3	14	1.4E+06	138.9
Srik	3036.77'	7817.93'	4.6	1.5	26.6	2.7E+06	185.1
Khur	3034.81'	7829.68'	0.24	1.7	34	3.4E+06	151.4
Vina	3033.99'	7839.33'	2.99	2.3	44.9	4.5E+06	134.8
Prat	3027.48'	7828.55'	0.28	2.7	46	4.6E+06	161.5
Surk	3024.67'	7817.34'	0.31	1.8	49	4.9E+06	183.8
Newt	3022.42'	7825.77'	0.104	1.8	54	5.4E+06	169.1
Chin	3024.59'	7844.70'	7.98	1.9	63.5	6.4E+06	140.4
Chan	3018.31'	7837.15'	3.65	2.0	66.9	6.7E+06	154.9
Sira	3007.92'	7838.03'	0.39	1.9	85	8.5E+06	159.5

Table 3(b) – Recorded on 11 January 2015

St. Code	Geographical Coordinates		Depth (km)	Mw	Epi Dist (km)	Hypo (cm)	Azi
	Latitude	Longitude					
Ayar	3018.22'	7825.91'	0.55	2.4	17	1.7E+06	93.9
Rajg	3024.59'	7844.70'	5.94	2.2	58.7	5.9E+06	358.6
Giya	3045.34'	7825.26'	7.19	2.3	51.5	5.2E+06	18.2
Srik	3036.77'	7817.93'	2.5	1.5	32.9	3.3E+06	7.6
Khur	3034.81'	7829.68'	6.14	1.7	37.5	3.8E+06	38.2
Vina	3033.99'	7839.33'	5.35	2.3	47.7	4.8E+06	54.0
Prat	3027.48'	7828.55'	4.01	2.3	26.7	2.7E+06	53.3
Surk	3024.67'	7817.34'	0.46	2.0	10.8	1.1E+06	18.2
Newt	3022.42'	7825.77'	0.84	2.3	17.98	1.8E+06	68.7
Chin	3024.59'	7844.70'	0.29	1.6	48	4.8E+06	77.3
Chan	3018.31'	7837.15'	1.18	2.2	34.98	3.5E+06	91.5
Sira	3007.92'	7838.03'	4.09	1.3	41.8	4.2E+06	118.8

Table 3(c) – Recorded on 24 January 2015

St. Code	Geographical Coordinates		Depth (km)	Mw	Epic Dist (km)	Hypo (cm)	Azi
	Latitude	Longitude					
Ayar	3018.22	7825.91	0.124	1.6	77	7.7E+06	142.0
Rajg	3024.59	7844.70	4.16	3.1	28.7	2.9E+06	91.7
Giya	3045.34	7825.26	0.31	3.0	47.4	4.7E+06	102.9
Srik	3036.77	7817.93	6.61	3.2	43.5	4.4E+06	127.4
Khur	3034.81	7829.68	1.04	1.8	61.2	6.1E+06	119.4
Vina	3033.99	7839.33	7.78	2.6	75.6	7.6E+06	114.6
Prat	3027.48	7828.55	8.23	2.6	67.5	6.8E+06	130.2
Surk	3024.67	7817.34	0.34	2.2	59.3	5.0E+06	145.3
Newt	3022.42	7825.77	5.32	3.2	70.8	7.1E+06	138.3
Chin	3024.59	7844.70	9.57	1.8	91.5	9.2E+06	122.2
Chan	3018.31	7837.15	1.33	2.0	88.99	8.9E+06	132.7
Sira	3007.92	7838.03	1.44	2.2	104	1.04E+07	139.9

4.2 Estimation of Source Parameters on 1 January, 2015

The digital data of 5 local earthquakes have been used to estimate earthquake source parameters. These small earthquakes were recorded at seismological laboratory, IIT Roorkee by both accelerogram and seismogram ~~have been considered~~ to compare the spectra. These earthquakes were recorded at 12 stations of seismological network at Tehri dam region. Source parameters consist of seismic moment, Brune stress drop, source radius and displacement. Source parameters are calculated by calculating spectral parameters.

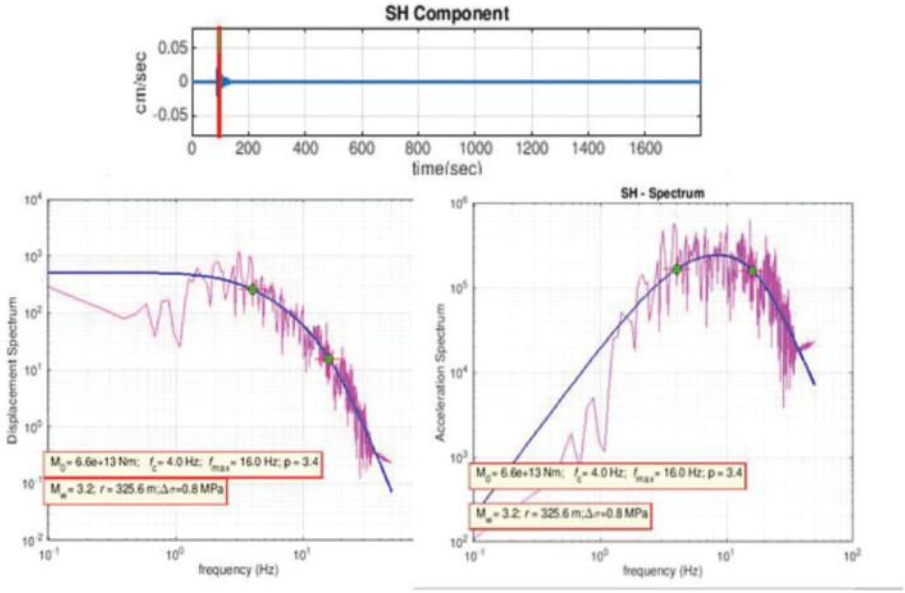

Fig. 2 - Observed displacement and acceleration spectra from SRIK station

Table 4(a) - Source parameters estimated from 12 Seismic stations for Local Earthquake recorded on Jan 1, 2015

St. Code	f_c (HZ)	f_{max} (HZ)	Mo (dyne cm)	Mω	R (m)	Δσ (bars)	$\Delta\sigma_{app}$ (bars)	D (cm)
Ayar	6.3	22.0	9.7E+19	2.6	205.3	5.0	1.54	0.25
Chan	13.2	15.6	1.3E+19	2.0	98.9	6.0	1.45	0.15
Chin	9.8	11.2	8.2E+18	1.9	133.5	2.0	1.64	0.05
Giya	5.9	14.5	3.6E+19	2.3	222.5	1.0	3.78	.08
Khur	12.4	16.7	4.7E+18	1.7	105.1	2.0	1.4	.046
Newt	11.7	19.7	5.7E+18	1.8	111.2	2.0	1.68	.05
Prat	4.2	9.7	1.2E+20	2.7	310.4	2.0	1.78	0.13
Rajg	16.4	20.0	2.2E+19	2.2	79.5	20.0	1.63	0.38
Sira	15.9	16.1	6.8E+18	1.9	81.9	5.0	1.94	0.11
Srik	20.0	28.3	2.2E+18	1.5	65.1	3.0	1.50	.05
Surk	15.6	21.6	6.4E+18	1.8	83.4	5.0	1.45	0.10
Vina	6.8	16.1	3.7E+19	2.3	190.7	2.0	1.37	0.11

Table 4(b) - Source parameters estimated from 12 Seismic stations for Local Earthqauke event recorded on 11 January, 2015

4	f_c (HZ)	f_{max} (HZ)	Mo (dyne cm)	Mω	R (m)	Δσ (bars)	$\Delta\sigma_{app}$ (bars)	D (cm)
Ayar	9.0	19.8	4.7E+19	2.4	145.1	7.0	1.59	0.24
Chan	14.3	18.6	2.6E+19	2.2	91.4	15	1.38	0.34
Chin	20.2	19.5	3.3E+18	1.6	64.5	5.0	1.45	0.08
Giya	6.8	14.1	3.0E+19	2.3	190.7	2.0	1.70	0.09
Khur	10.7	21.0	4.0E+18	1.7	121.3	1.0	1.65	0.029
Newt	14.2	19.9	3.2E+19	2.3	92.1	18	1.59	0.41
Prat	5.3	19.4	3.4E+19	2.3	247.2	1.0	1.5	0.06
Rajg	6.0	14.1	2.2E+19	2.2	218.8	1.0	1.63	0.05
Sira	27.2	28.3	1.1E+18	1.3	47.8	5.0	1.52	0.05
Srik	21.5	27.7	1.7E+18	1.5	60.7	3.0	1.94	0.05
Surk	29.2	21.5	1.2E+19	2.0	88.4	7.0	1.57	0.16
Vina	18.6	29.2	4.5E+18	1.7	139.0	1.0	1.46	0.025

Table 4(c) - Source parameters estimated from 12 Seismic stations for Local Earthquake recorded on Jan 24, 2015

St. Code	f_c (HZ)	f_{max} (HZ)	Mo (dyne cm)	Mω	R (m)	Δσ (bars)	$\Delta\sigma_{app}$ (bars)	D (cm)
Ayar	13.0	23.2	3.0E+18	1.6	100.4	1.0	1.6	0.03
Chan	12.6	14.0	1.1E+19	2.0	103.5	4.0	1.7	0.11
Chin	13.5	16.2	6.3E+18	1.8	96.7	3.0	1.52	0.07
Giya	7.7	12.6	3.4E+20	3.0	169	31	1.67	1.30
Khur	11.5	39.6	5.1E+18	1.8	113.1	2.0	1.88	0.04
Newt	2.0	20.3	6.6E+20	3.2	667.4	1.0	1.77	0.16
Prat	8.5	9.7	9.2E+19	2.6	153.4	11.0	1.63	0.43
Rajg	8.9	16.4	4.5E+20	3.1	146.7	63.0	1.86	2.3
Sira	13.4	16.6	2.6E+19	2.2	97.4	12.0	1.38	0.30
Srik	4.0	16.0	6.6E+20	3.2	325.6	8.0	1.77	0.68
Surk	15.8	18.4	2.0E+19	2.2	82.4	15.0	1.8	0.32
Vina	8.9	16.4	8.6E+19	2.6	146.7	12.0	1.74	0.43

5. RESULTS AND DISCUSSIONS

Different graphs were plotted to study the properties of the source parameters and their relationship. These plots are described in detail below:

5.1 Seismic Moment vs Corner Frequency

Corner frequency varies inversely with the source size i.e., it decreases as the source size increases.

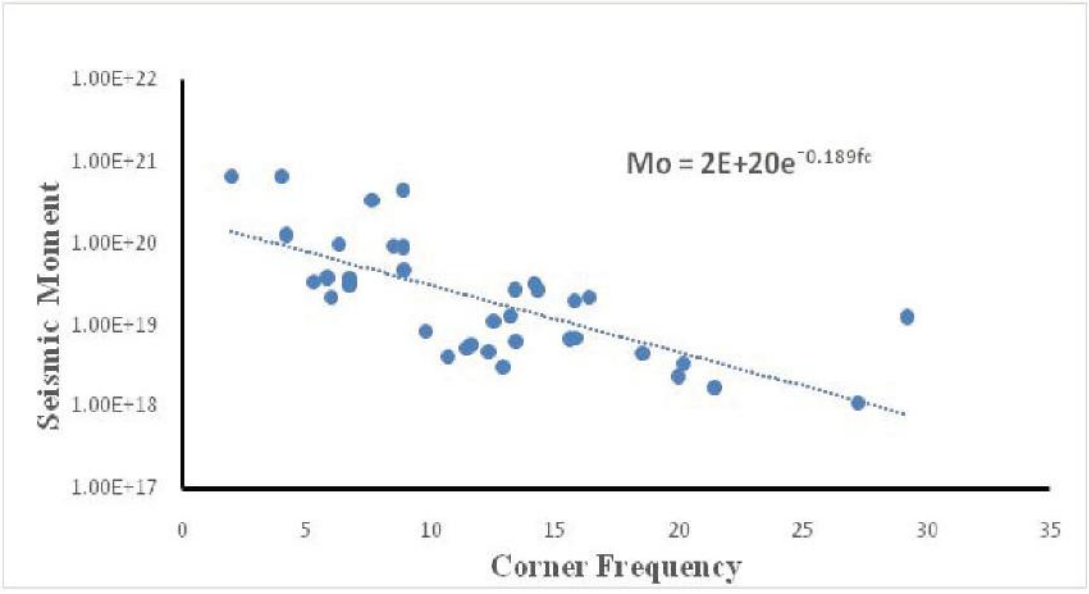

Fig. 3 - Plot between corner frequency and seismic moment

The trend line shows linear variation and the relationship between Seismic moment and corner frequency is as follows:

$$M_0\,(\text{dyne-cm}) = 2.0\text{x}10^{20}\, e^{-0.189\, fc} \qquad (7)$$

The present study on Tehri dam site does not agree with the standard relations on this site, mainly because of different range of magnitudes taken by the researcher for estimating these scaling laws.

5.2 Brune stress drop Vs Seismic Moment

The plot between Brune stress drop and seismic moment shows a linear variation i.e Brune stress drop increases as seismic moment increases and the relationship between seismic moment and corner frequency is as follows:

$$\Delta\sigma(\text{bars}) = 7\text{E-}05M_0^{\,0.2473} \qquad (8)$$

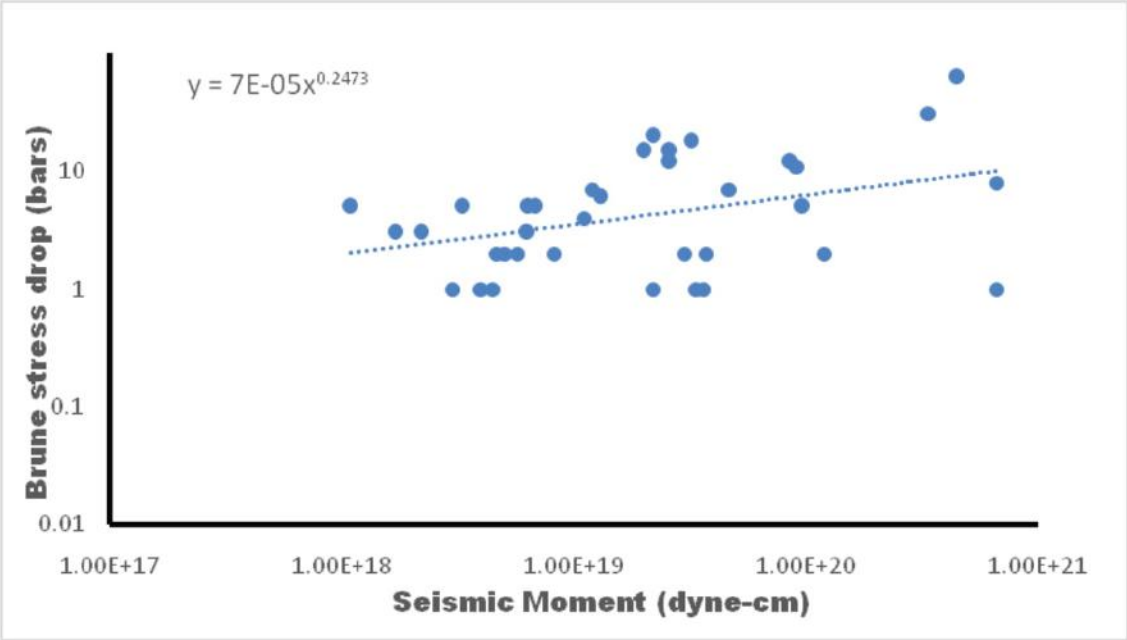

Fig. 4 - Plot between Brune stress drop and seismic moment

5.3 f_{max} Vs Seismic Moment

Plot between f_{max} and seismic moment is depicted to carry out the relationship between f_{max} and source size. f_{max} is obtained from acceleration spectra of local earthquakes. According to the study of the Tehri dam site f_{max} varies from 9.7 Hz to 39.6 Hz. This variation is because of the possible reason as indicated by which f_{max} varies because of local geological structure below the recording station (Hanks, 1982). f_{max} almost shows the similar trend as *fc*. It shows the decrease with decrease in seismic moment. From the studies it seems f_{max} also have some relation with size of source.

The relationship between f_{max} and seismic moment is as follows:

$$f_{max} = 1.032\ \text{E+}03 \quad M_o^{-0.0} \qquad (9)$$

5.4 Corner frequency *fc* vs Seismic Moment

The equation between f_c and seismic moment obtained from the best fit line in Fig. 6 is as follows:

$$f_c = 1.0E+06\ M_0^{-0.262} \quad (10)$$

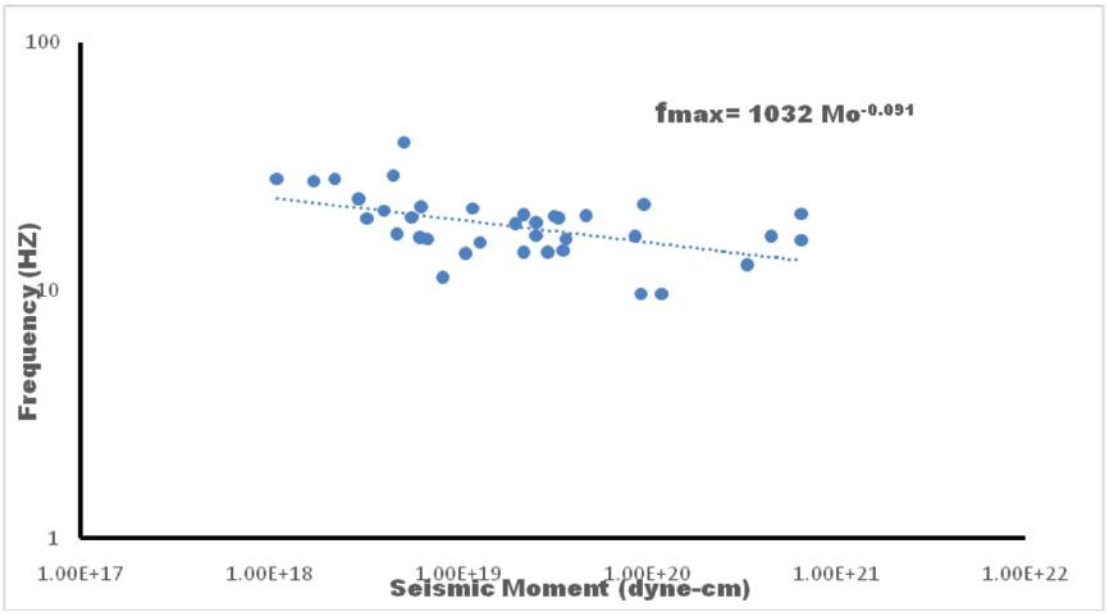

Fig. 5 - Plot between f_{max} and seismic moment

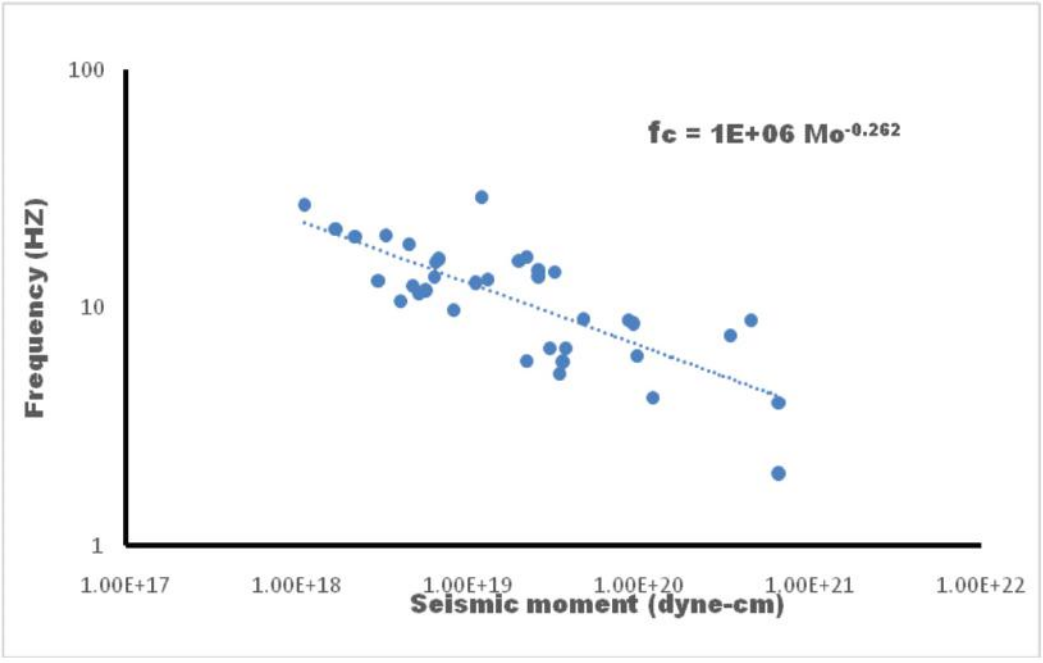

Fig. 6 - Plot between f_c and seismic moment

5.5 Seismic Moment vs Source Radius

From the plot between seismic moment and source radius (Fig. 7), it is observed that apart from some scattering, source radius tends to increase with increase in seismic moment. The plot depends on reading which is taken by 12 recording stations placed in Tehri dam region of different local earthquake events of magnitude ranges from (M_w) of 1.3 to 3.2. Seismic moment varies from 2.2x 10^{18} dyne-cm to 6.6x10^{20} dyne-cm.

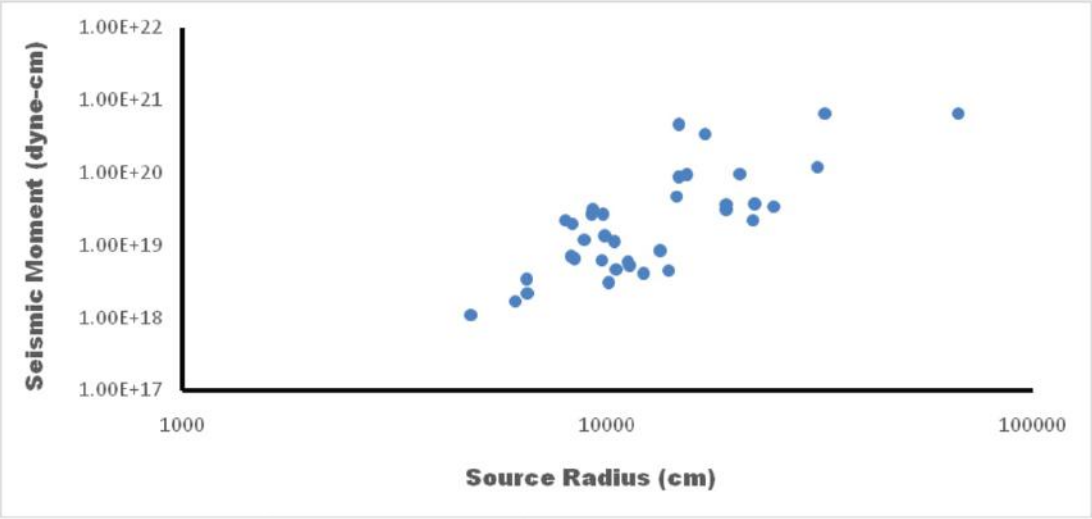

Fig. 7 - Plot between seismic moment and source radius

6. SUMMARY

The Tehri Project, basically provided irrigation and hydroelectric project, was completed in 2005, and the reservoir filling process started instantly after it. The dam construction was almost unrelated to the magnitude of the Uttarkashi earthquake (M = 6.8) on October 20, 1991. R.I.S. is considered to be beneficial for seismic stability of high earth dams.

The area experiences frequent earthquakes just immediately after the Uttarkashi and, the Chamoli earthquake (M = 6.6) happened on 29 March, 1999. Therefore, in order to address concerns about the safety of dams in the event of a major earthquake, estimation of source parameters for the events occurring in this region is necessary for safety of dam structures and their operations. However, importance of India's seismic source parameters began between mid-1990s introduced a local advanced telemetry cluster at Garhwal Lesser Himalaya. Several efforts have been made from digital data of local earthquakes in the Garhwal and Kumaon regions of the Himalayas. Numerous efforts have been made to calculate the source parameters of the earthquake in India (Tandon and Srivastava, 1974) which successfully estimated stress drop and mean displacements of several earthquakes ($5.0 \leq M \leq 8.5$) in India. In this study, estimation of the source parameters of 3 small local events ($1.3<Mw<3.2$) occurred in the Tehri dam region have been investigated with detailing of local earthquake data used for estimation of hypocenter parameters. The last section (Figs. 3, 4, 5, 6, and 7) as well as Tables 3 and 4 involve various characteristics of estimated source parameters like f_{max} followed by development of the scaling law for the region.

Further, the dynamic settlement of the earth dam is estimated to be well within safe limit during a major design earthquake.

7. CONCLUSIONS

From the above study on estimation of source parameter of local earthquake events in Tehri dam region, following have been drawn:

- Seismic moment ranges from $2.2x10^{18}$ dyne-cm to $6.6x10^{20}$ dyne-cm. For these seismic moments values the values for corner frequency f_c and f_{max} vary from 4 Hz to 20 Hz and 16 Hz to 28.3 Hz respectively.
- The source radius of the above events ranges from 65.1 m to 667.4 m and source size increases as seismic moment of earthquake increases.
- The relationship between seismic moment and corner frequency has been developed for the region as: M_0 (dyne-cm) = $2.0 \times 10^{20} e^{-0.189 f_c}$
- Brune stress drop ranged from 1 bar to 63 bars.
- The change in Brune's stress drop shows a trend of increased maximum envelope with focal depth and is clearly associated with the strength of the crust.
- The Corner frequency f_c follows the decreasing trend with the seismic moment. The relationship between Corner frequency and seismic moment has been developed as: $f_c = 1.0E+06M_o^{-0.262}$
- The f_{max} also follows the same decreasing trend with seismic moment similar to f_c.
- The relationship between f_{max} and seismic moment has been derived as: $f_{max} = 1.032\ E+03M_o^{-0.091}$.
- This study suggests that there shall be no major earthquake near Tehri. Also it seems that Tehri dam is safe.

ACKNOWLEDGEMENTS

This is the parts of the master thesis work. Authors are indebted to the Head, Department of Earthquake Engineering, IIT Roorkee, Roorkee for providing excellent computational facilities. The conclusion drawn is the sole responsibility of the authors only, not necessarily the institute.

References

Aki, K. (1966). Generation and propagation of G waves from the Niigata earthquake of June 16, 1964, Part 2: Estimation of earthquake moment, released energy, and stress strain drop from the G wave spectrum, Bull. Earthq. Res. Inst. 44, 73–88.

Brune, J. N. (1970). Tectonic stress and the spectra of seismic shear waves from earthquake, J. Geophys. Res. 75, 4997-5009.

Choudhury, Swapnamita, Param Gautam, and Paul, Ajay (2013). Seismicity and reservoir induced crustal motion study around the Tehri Dam, India, Acta Geophysica, 61 (4), 923-934.

Finn, W. D. L. (1993). Seismic design considerations for dams in Himalaya with references to Tehri dam, In: earthquake hazard and large dams in the himalaya, ed.V K Gaur, INTACH, NewDelhi, 116–134 Hanks, T.C. (1982). fmax. Bull Seismol Soc Am 72: 1867–1879.

Hanks, T. C. (1982). fmax, Bulletin of Seismological Society of America 72, 1867-1879.

Havskov, J. and Ottemoller, L. (2000). SEISAN Earthquake Analysis Software. Seismological Research Letters, 70, 532-534.

Keile,s-Borok, V. (1959). An estimation of the displacement in an earthquake source and of source dimensions, Ann. Geofis. (Rome) 12, 205 214.

Kumar, Ashwani; Kumar, Arjun; Gupta, S.C., Mittal, Himanshu; Kumar, Rohtash (2013a). Source parameters and f_{max} in Kameng region of Arunachal Lesser Himalaya, Journal of Asian Earth Sciences. 70-71, 35-44.

Kumar, Ashwani; Kumar, Arjun; Gupta, S. C., Jindal, A. K. and Ghangas, Vandana (2013b).

Seismicity and source parameters of local earthquakes in Bilaspur region of Himachal Lesser Himalaya, Arabian Journal of Geosciences. 7(6), 2257-2267.

Kumar, Rohtash; Gupta, S. C., Kumar, Arjun and Mittal, Himanshu (2015). Source parameters and f_{max} in lower Siang region of Arunachal lesser Himalaya, Arabian Journal of Geosciences, 8(1), 255-265

Lienert, B., Berg, E. and Frazer, N. (1986). An earthquake location method using centred, scaled and adaptively damped least squares, Bulletin of the Seismological Society of America 76(3): 771-783.

Nakano, H. (1923). Notes on the nature of the forces which give rise to the earthquake motions, Seismological Bulletin of Central Metrological Observatory of Japan, 1, 92–120.

O'Neill, M. E. and Healy, J. H. (1973). Determination of source parameters of small earthquakes from P-wave rise time, Bull. Seism. Soc. Am., 63 (2), 599-614.

Paidi,Vinod, Kumar, Ashwani; Gupta, S.C. and Kumar, Arjun (2015). Estimation of source parameters of local earthquakes in the environs of Koldam site, Arabian Journal of Geosciences 8(1), 227-238.

Sengupta, A. (2010). Estimation of permanent displacements of the Tehri dam in the Himalaya due to future strong earthquakes, Sadhana, 35 (3), 373–392.

Tandon, A. N., and Srivastava, H. N. (1974). The stress drop and average dislocation of some earthquakes in the Indian sub-continent, Pure and Applied Geophysics, 112 (6), 1051–1057.